Journal of Catalysis 365 (2018) 391–404

Contents lists available at ScienceDirect

Journal of Catalysis

journal homepage: www.elsevier.com/locate/jcat

The mechanism of ethanol steam reforming on the Co^0 and Co^{2+} sites: A DFT study

Meng-Ru Li[a], Gui-Chang Wang[a,b,*]

[a] College of Chemistry, Key Laboratory of Advanced Energy Materials Chemistry (Ministry of Education) and Synergetic Innovation Center of Chemical Science and Engineering (Tianjin), Nankai University, Tianjin 300071, People's Republic of China
[b] State Key Laboratory of Coal Conversion, Institute of Coal Chemistry, Chinese Academy of Sciences, Taiyuan 030001, People's Republic of China

ARTICLE INFO

Article history:
Received 8 February 2018
Revised 18 May 2018
Accepted 1 July 2018

Keywords:
ESR reaction
Reaction mechanism
Co(0 0 0 1)
CoO(1 0 0)
Active sites
Density functional theory calculations

ABSTRACT

It is well known that Co catalysts are efficient for ethanol steam reforming (ESR) reactions, but whether the active site is Co^0, Co^{2+}, or Co^0–Co^{2+} is still debated. In the present work, density functional theory calculations are performed to study the reaction mechanisms of ESR over Co^0, Co^{2+}, and Co^0–Co^{2+} sites. The mechanism of ESR on Co^0 sites is $CH_3CH_2OH \rightarrow CH_3CH_2O \rightarrow CH_3CHO \rightarrow CH_3CO \rightarrow CH_3 + CO$, and H_2 is formed by the combination of adsorbed H species with a relatively high barrier (1.37 eV). On the CoO (1 0 0) surface, the main product CH_3CHO is produced through the consecutive dehydrogenation of ethanol, but the CoO surface lacks the C–C bond activation that ESR requires. On Co catalysts with a combination of Co^0 and Co^{2+} (Co_{10}/CoO(1 0 0) model), a strong synergetic effect was found: On interface, it occurs through the path $CH_3CH_2OH \rightarrow CH_3CH_2O \rightarrow CH_3CHO \rightarrow CH_3CO$, the resulting CH_3CO on interface will spread to Co_{10} cluster and bind to OH on the interface which results from H_2O dissociation on the CoO surface: $CH_3CO \rightarrow CH_3COOH$ (interface), and the resulting acetic acid (CH_3COOH) will spread to the Co_{10} cluster and go on C—C scission with the path $CH_3COOH \rightarrow CH_3 +$ *trans*-COOH $\rightarrow CH_3 + CO_2 + H$ to form CO_2. On CoO parts (Co^{2+} sites), H_2O dissociation is more facile than that on Co^0 sites, and the formed OH (or O) migrates to the interface easily and reacts with CH_x species to release carbon deposition. On the interface between Co^0 and Co^{2+}, some key coupling reactions related to ESR are favored, such as H_2 formation, the formation of CH_3COOH, and the oxidation of CH_x species to release coke formation, thus leading to high activity for ESR. Possible reasons for the result that C—C bond breaking can take place on Co^0 sites instead of Co^{2+} sites have been analyzed, and it was found that Co^0 sites with a large ensemble size of Co favor dissociation reactions such as C—C scission. Based on the present work, it is expected that a proper catalyst for ESR reactions should have metallic sites with large ensemble size to break C—C bonds and oxidized metal sites with small ensemble size to favor water dissociation as well as acetate species formation.

1. Introduction

Both rising global energy demands and serious environmental problems call for the replacement of petroleum-based fuels with alternative fuels. Hydrogen, a promising environmentally friendly energy source, has attached much attention [1]. To date, ethanol steam reforming (ESR) stands out among numerous hydrogen production technologies such as the steam reforming of methane [2] and the steam reforming of methanol [3-5] for high selectivity for H_2 [6]. The renewable fermentation of biomass synthetic route, the advantage in storage facilities, handling, and transport safety, and feasible H_2 production applying in the fuel cell, makes ESR more efficient in application in direct biorenewable resources and in fuel cells as storage media [7,8]. The strongly endothermic ESR calls for a continuous heat supply at low temperature in production, and requires an efficient catalyst for ESR. The noble metal catalysts (Pt [9], Pd [10], Rh [11], Ir [12], and Ru [13]) have shown catalytic activity toward ESR. However, the low H_2 yield at low temperature, high methane selectivity, and high cost have limited the application of noble-metal-based catalysts. On the other hand, non-noble Co-based catalysts could obtain a low propensity to catalyze carbon deposition with low selectivity of byproducts [14]. The supports (CeO_2, ZnO, MgO, Al_2O_3, zeolites-Y, TiO_2, SiO_2, $La_2O_2CO_3$, CeO_2–ZrO_2) play a vital role in their catalytic activity, selectivity,

---

* Corresponding author at: College of Chemistry, Key Laboratory of Advanced Energy Materials Chemistry (Ministry of Education) and Synergetic Innovation Center of Chemical Science and Engineering (Tianjin), Nankai University, Tianjin 300071, People's Republic of China.

E-mail address: wangguichang@nankai.edu.cn (G.-C. Wang).

https://doi.org/10.1016/j.jcat.2018.07.002

and carbon deposition [15]. Acid supports such as Al_2O_3 strongly facilitate carbonaceous deposition by the dehydration of ethanol. In contrast, support oxides of a basic nature lead to the condensation of ethanol to higher oxygenates [16,17]. The only weakly basic reducible metal oxides such as CeO_2 and ZrO_2 turn to be the most suitable support for ESR, owing to their high oxygen storage capacity and oxygen mobility [18], The active sites on reducible-metal-oxide supported Co catalyst for ESR are combinations of Co^0 and Co^{2+} sites [19]. Del Río et al. [20] have suggested that the CoO_x ($x < 2$) phase is needed to obtain sufficient CO_2 and H_2 selectivity. Turczyniak et al. [21] have reported the presence of Co(II) and metallic Co under higher pressure (4–20 mbar) of ethanol/water on Co/CeO_2 and gains high CO_2 selectivity and H_2 yield.

Theoretically, numerous studies on the mechanisms of ethanol decomposition/oxidation on metals [22–27] and metallic oxides [28–31] have been carried out by density functional theory (DFT) calculations. Computational investigation on ESR on the Co(0 0 0 1) surface has revealed that the mechanisms of ESR involve the subsequent dehydrogenation of ethanol, C—C scission, the dissociation of water, and water-gas shift reactions [32]. However, DFT calculation on ESR mechanisms on Co catalysts with both Co^0 and Co^{2+} sites is lacking. Here, we initially use the Co(0 0 0 1) surface and the CoO(1 0 0) surface to simulate the ESR reactions on Co^0 and Co^{2+} sites. Furthermore, we develop a mixed model with Co(0 0 0 1) and CoO(1 0 0) surfaces to explore the ESR mechanism on the mixed CoO_x surface in the Co catalyst based on a reducible support in the report from Turczyniak et al. [21].

2. Calculation methods and models

2.1. Methods

The Vienna ab initio simulation package (VASP) [33–35] was applied to investigate the ethanol reaction on the Co^0 and Co^{2+} sites by self-consistent periodical DFT calculations with projected augmented wave (PAW) [36] pseudopotentials. All the electronic structures were calculated using the Perdew–Burke–Ernzerhof (PBE) [37] form of the generalized gradient approximation (GGA) expanded in a plane wave basis with a kinetic cutoff energy of 400 eV. The climbing image general nudged elastic band (CI-NEB) [38] method was employed to locate the transition states (TSs). Spin polarization was included in the calculations. The adsorption energy (E_{ads}), activation energy (E_a), and reaction energies (ΔE) were calculated by the following three formulas: $E_{ads} = E_{A/M} - E_A - E_M$, $E_a = E_{TS} - E_{IS}$, and $\Delta E = E_{FS} - E_{IS}$, respectively. Here, E_A, E_M, $E_{A/M}$, E_{TS}, E_{IS}, and E_{FS} mean the calculated energies of the adsorbate, substrate, adsorption system, transition state, initial state (IS), and final state (FS), respectively.

2.2. Models

The Co(0 0 0 1) surface containing the Co^0 site was modeled by the p (3 × 3) unit cell of four layers, of which the uppermost two layers were relaxed as established in Fig. 1a. A vacuum space of 15 Å was applied in the case of the spurious interactions normal to the surface. A 3 × 3 × 1 Monkhorst–Pack k-point mesh [39] was used in the surface Brillouin zone. The CoO(1 0 0) surface shown in Fig. 1b, containing Co^{2+}, was modeled by a p (3 × 2) unit cell of four layers that were separated by a 15 Å vacuum with the 2 × 3 × 1 Monkhorst–Pack k-point mesh. The uppermost two layers were allowed to relax to optimize the structures. The experimental CoO lattice constant was applied (4.261 Å) [40,41].

For the model with Co^0 and Co^{2+} sites, a two-layer Co_{10} cluster modeled in the Co(0 0 0 1) surface was set on a larger p (2 × 6) unit cell of the CoO(1 0 0) surface with four layers. The top layer of the Co_{10} cluster possesses four Co atoms, and the second layer of the Co_{10} cluster, containing six Co atoms, interacts with the CoO(1 0 0) surface through Co in the Co_{10} cluster and lattice oxygen on the surface. The vacuum space of 15 Å was applied in the case of the spurious interactions normal to the surface shown in Fig. 1c with the 3 × 1 × 1 Monkhorst–Pack k-point mesh. The upper two layers of CoO(1 0 0) and the Co_{10} cluster were relaxed. The Coulomb (U) and exchange (J) interactions were taken into consideration due to the highly correlated electronic states of the cobalt oxide CoO. The GGA+U [42,43] method was used to recover the effect of 3d electron correlation on the 3d transition metal oxide CoO with the set $U - J = 3.3$ eV [44]. For the charge distribution of different sites (Co_{10} cluster, CoO surface and interface) in the Co_{10}/CoO(1 0 0) model, as shown in Fig. 2, the Co_{10} cluster donates electrons to the lattice oxygen on the CoO surface, leading to the charge of Co on the interface being $+x$ ($0 < x < 2$). As a result, the interface can be denoted as Co^{x+} sites ($0 < x < 2$).

3. Results

3.1. Adsorption of pertinent species

To get the difference of adsorption properties of the intermediates on Co^0 and Co^{2+} sites, we compare the adsorption configurations and energies for the main species involved in ESR reactions on the Co(0 0 0 1) surface with that on the clean CoO(1 0 0) surface. The corresponding configurations on Co(0 0 0 1) and CoO(1 0 0) surfaces were displayed in Fig. S1 in the Supporting Information. It is found that the adsorption energies of the main species on Co (0 0 0 1) are higher than those on CoO(1 0 0), indicating the stronger interaction between the main species and the Co^0 site. The stronger interaction between carbon species and the Co^0 site is in accordance with the higher electron density of metallic Co. For the adsorption on Co_{10}/CoO(1 0 0) model shown in Fig. 3, the most preferred adsorption site for most carbon species in the Co_{10}/CoO (1 0 0) model is the Co_{10} cluster, followed by the interface and the CoO(1 0 0) surface. The highest adsorption energies of intermediates on the Co_{10} cluster are caused by the higher unsaturation of Co and the higher density of Co sites. In addition, the species CH_3 and CO tend to get adsorbed onto the Co_{10} cluster stably, and could hardly be adsorbed on the interface.

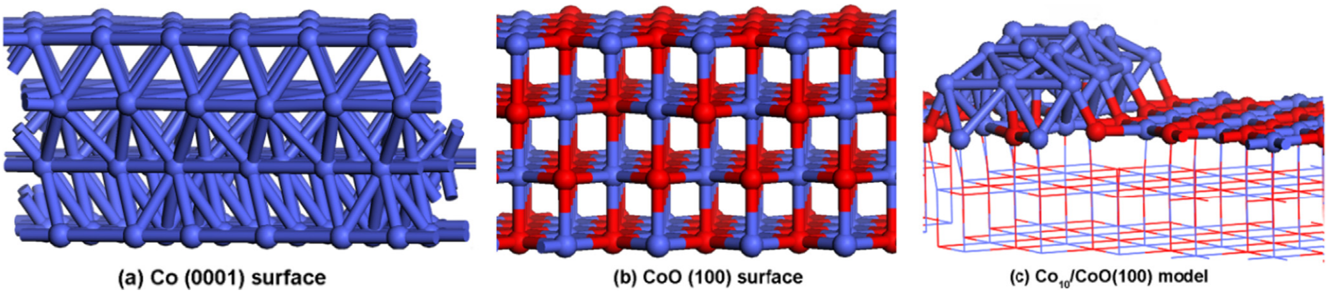
(a) Co (0001) surface
(b) CoO (100) surface
(c) Co_{10}/CoO(100) model

Fig. 1. Structures of Co(0 0 0 1) (a), CoO(1 0 0) surface (b), and Co_{10}/CoO(1 0 0) model (c).